

Supporting Information

Ti₃C₂T_x MXene-based hybrid nanocoating towards flame retardant, fire early-warning and piezoresistive tension sensing smart polyester fabric

Menghan Guo^a, Wenqing Wang^{a, b*}, Bin Zhai^c, Jingtao Li^a, Liran Zhang^{a, b}, Jingchun Li^a, Kexin Luo^a, Rui Wang^{a, b}

^aMaterials Design & Engineering Department, Beijing Institute of Fashion Technology, Beijing 100029, China

^bBeijing Key Laboratory of Clothing Materials R&D and Assessment, Beijing Engineering Research Center of Textile Nanofiber, Beijing Institute of Fashion Technology, Beijing 100029, China

^cNo.5 Geological Brigade of Shandong Provincial Bureau of Geology and Mineral Resources, Taian, Shandong 271000, China

*20180021@bift.edu.cn

Content

Fig.S1. Photos of the fire warning device (a) and heating plate (b).	3
Fig.S2. Q-MXene suspension for different days.	3
Fig.S3. SEM-EDS mapping images of the (a) FPP, (b) FPP@AM-3, (c) FPP@PM-3 and (d) FPP@A5-M1 for the chosen zone.	3
Fig.S4. High resolution XPS spectra of P 2p region on (a) FPP@AM-3, (b) FPP@PM-3, and (c) FPP@A5-M1.	4
Fig.S5. TG (a) and DTG (b) curves for FRPET, FPP, FPP@PM-3, FPP@AM-3, and FPP@A5-M1.	4
Fig.S6. The weight loss with washing time increasing for modified FPP fabric.	4
Fig.S7. Initial, ignition and extinguishing times of FPP fabric.	5
Fig.S8. Limiting oxygen values for FRPET and FPP@A5-M1.	5
Fig.S9. Thermal infrared images of FRPET, FPP@PM-3, FPP@AM-3 and FPP@A5-M1 fabric at different combustion time.	6
Fig.S10. MXene-based fabric Cone Volume Data. presented (a) pHRR and (b) TSP curves.	7
Fig.S11. The char residual (a) SEM and (b) Raman plots of FPP fabric.	7
Fig.S12. FPP@A5-M1 carbon residue resistance.	8
Table S1. The EDS elemental content of modified FRPET fabric.	9
Table S2. The value of ΔU at $\Delta T=130$ °C for FPP@A5-M1.	9
Table S3. Cone calorimeter test for pristine FRPET and its modified fabric.	9

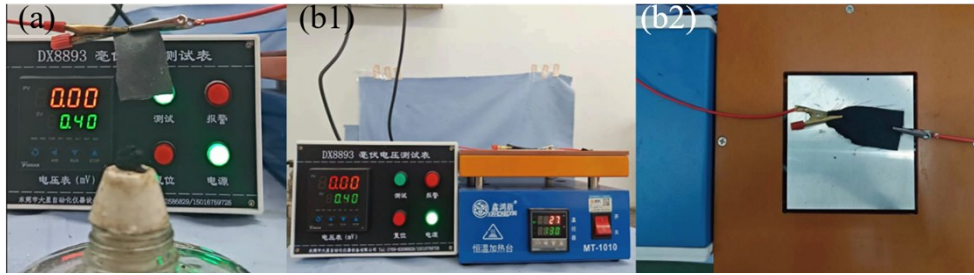


Fig.S1. Photos of the fire warning device (a) and heating plate (b).

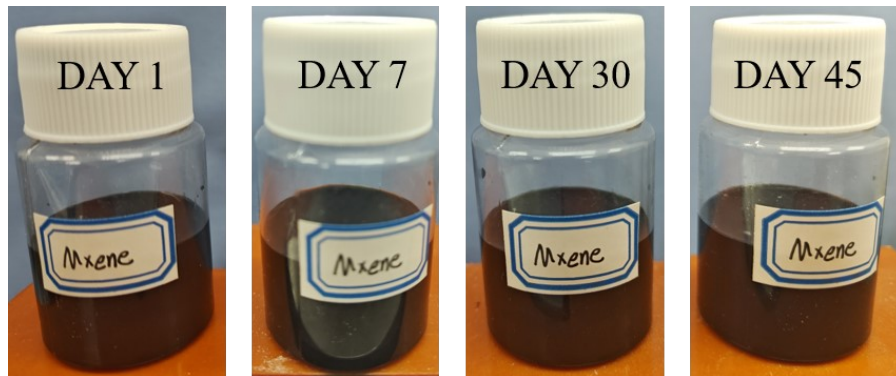


Fig.S2. Q-MXene suspension for different days.

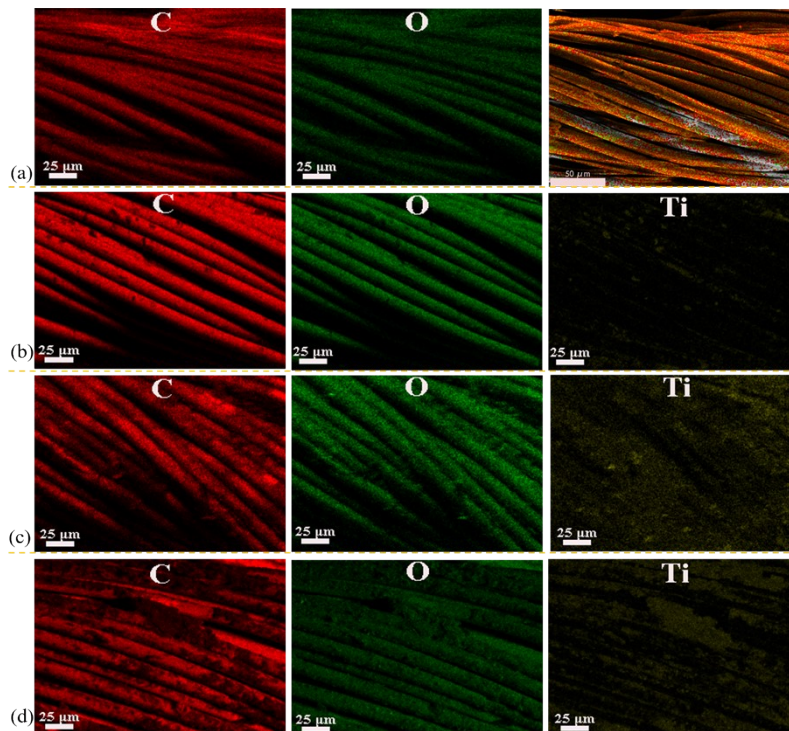


Fig.S3. SEM-EDS mapping images of the (a) FPP, (b) FPP@AM-3, (c) FPP@PM-3 and (d) FPP@A5-M1 for the chosen zone.

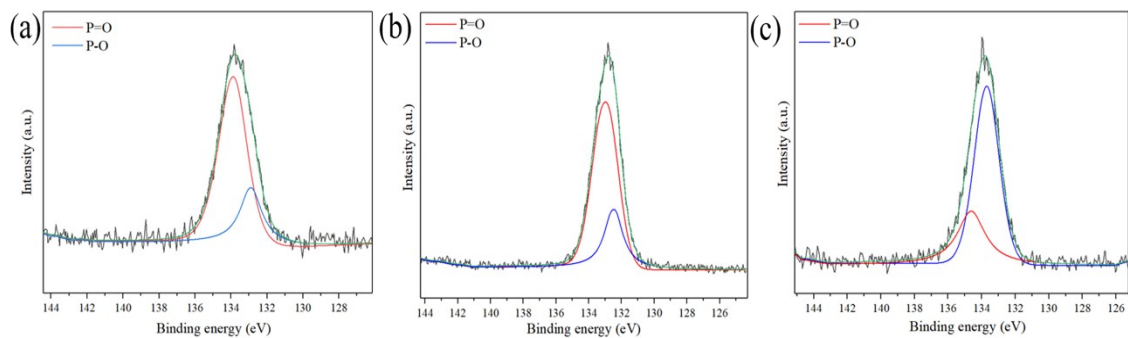


Fig.S4. High resolution XPS spectra of P 2p region on (a) FPP@AM-3, (b) FPP@PM-3, and (c) FPP@A5-M1.

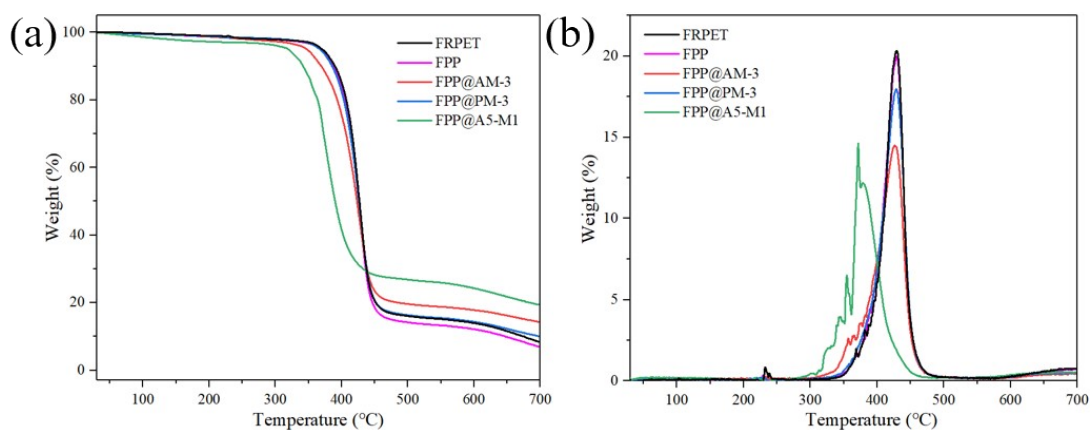


Fig.S5. TG (a) and DTG (b) curves for FRPET, FPP, FPP@PM-3, FPP@AM-3, and FPP@A5-M1.

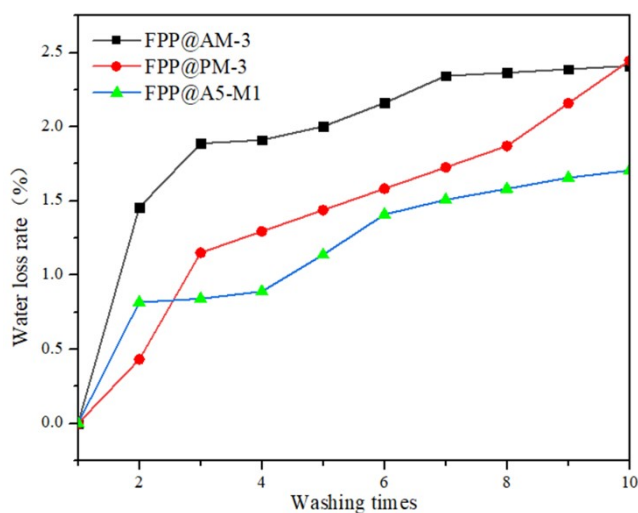


Fig.S6. The weight loss with washing time increasing for modified FPP fabric.

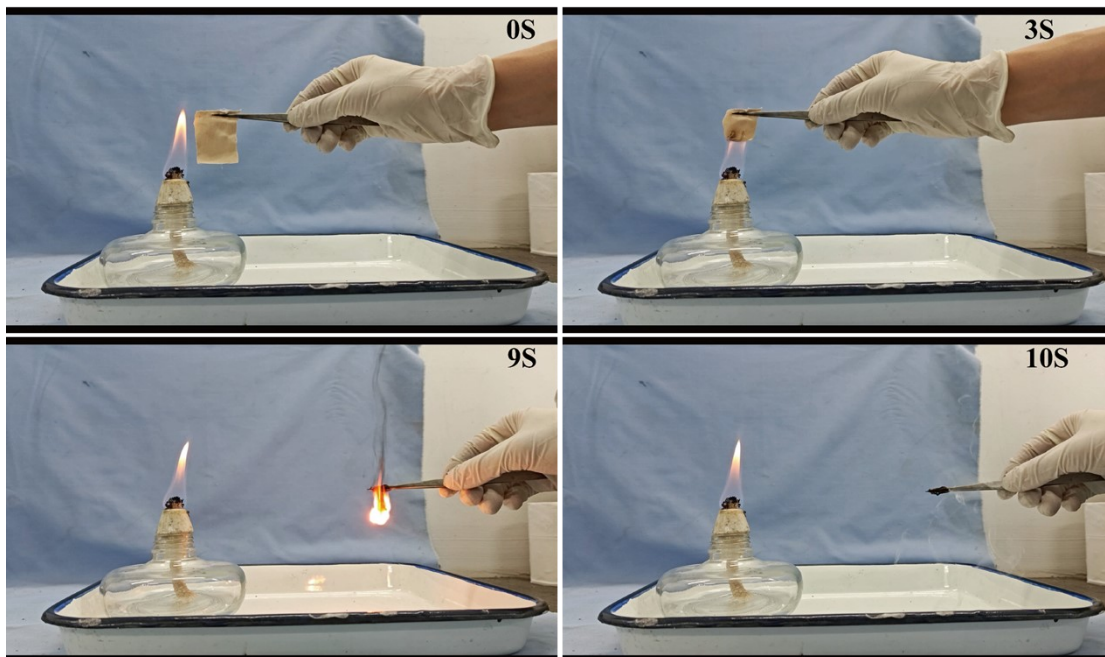


Fig.S7. Initial, ignition and extinguishing times of FPP fabric.

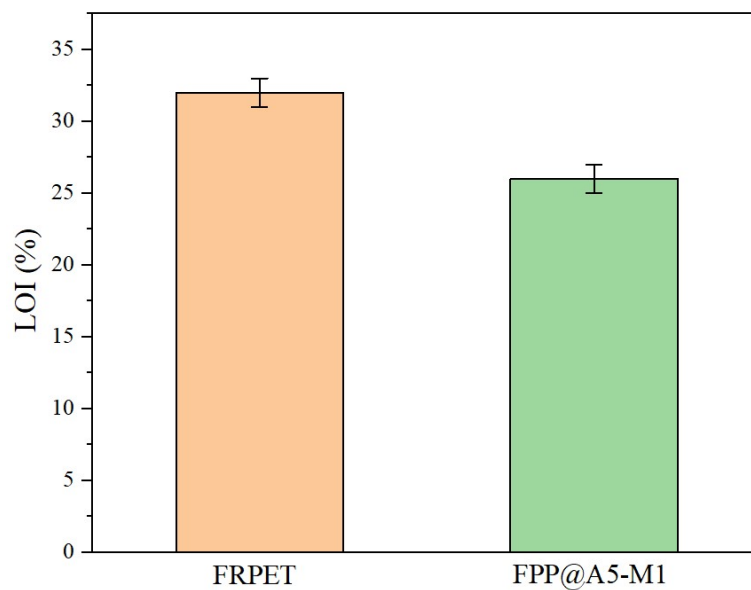


Fig.S8. Limiting oxygen values for FRPET and FPP@A5-M1.

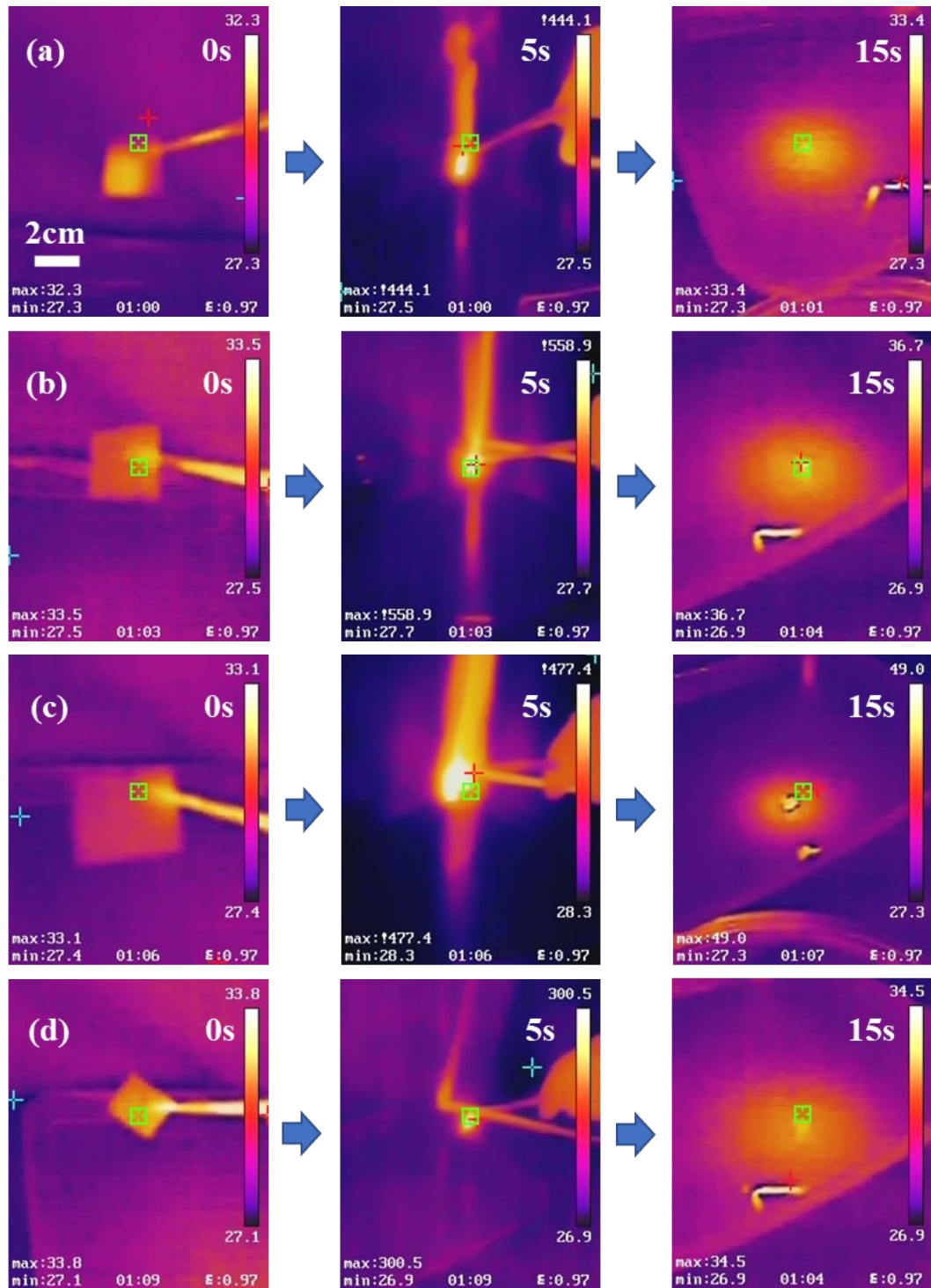


Fig.S9. Thermal infrared images of FRPET, FPP@PM-3, FPP@AM-3 and FPP@A5-M1 fabric at different combustion time.

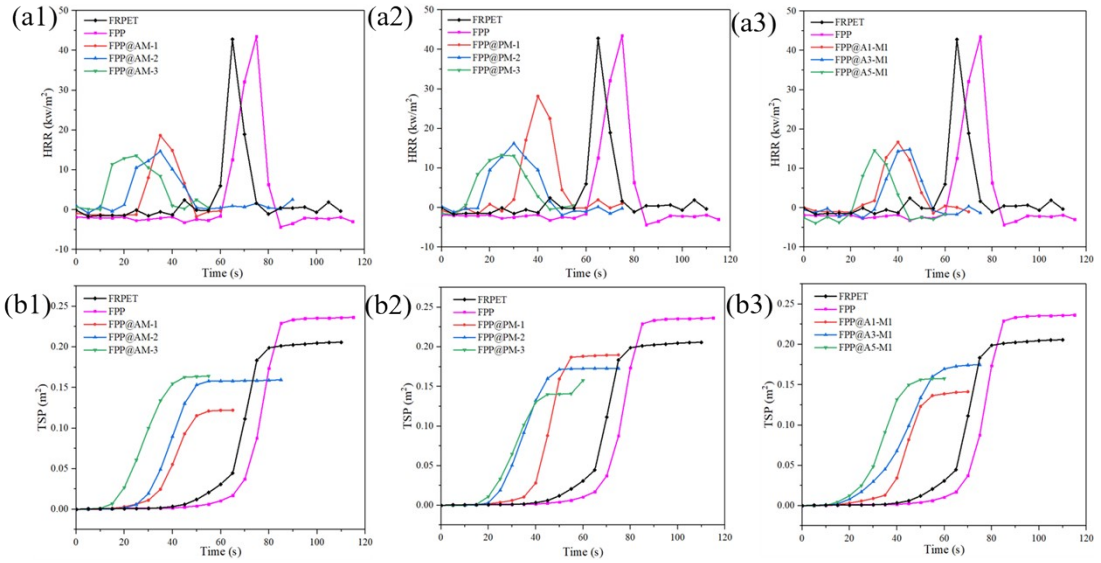


Fig.S10. MXene-based fabric Cone Volume Data. presented (a) pHRR and (b) TSP curves.

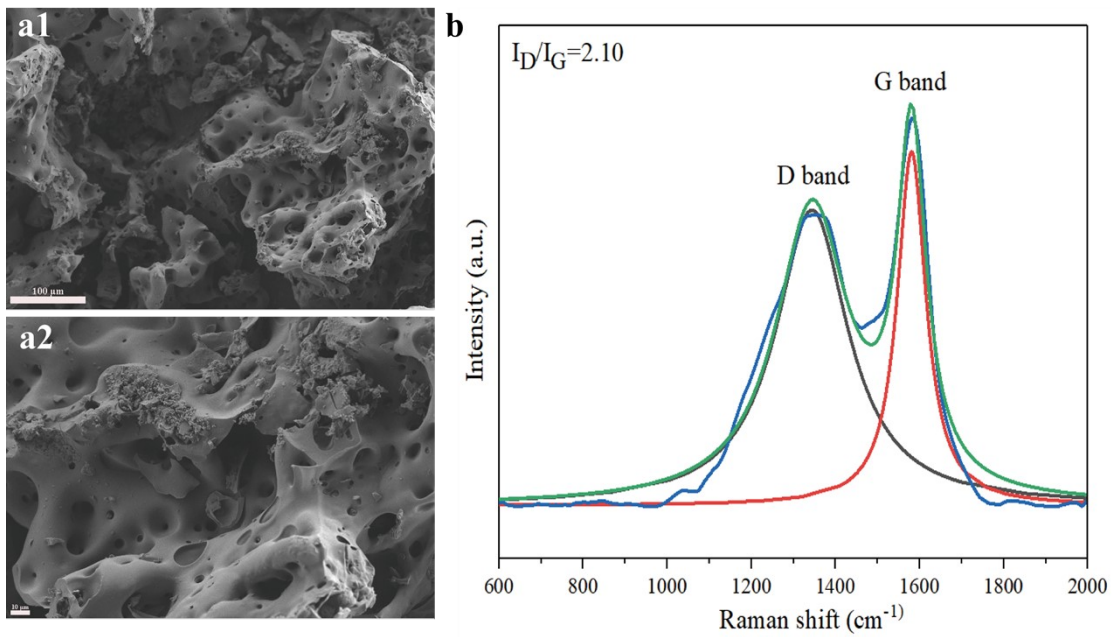


Fig.S11. The char residual (a) SEM and (b) Raman plots of FPP fabric.



Fig.S12. FPP@A5-M1 carbon residue resistance.

Table S1. The EDS elemental content of modified FRPET fabric.

Sample	FPP@AM-3	FPP@PM-3	FPP@A5-M1
carbon content (%)	57.5	42.63	61.96
Phosphorus content (%)	3.95	11.69	3.92

Table S2. The value of ΔU at $\Delta T=130$ °C for FPP@A5-M1

Washing times	1	2	4	6
ΔU (mV)	0.48	0.46	0.34	0.35

Table S3. Cone calorimeter test for pristine FRPET and its modified fabric.

Sample	TTI	PHRR (KW/m ²)	THR (MJ/m ²)	TSP (m ²)
FRPET	67	18.93	0.2112	0.1567
FPP	66	43.47	0.4412	0.2192
FPP@PM-1	37	28.17	0.3072	0.1489
FPP@PM-2	21	16.25	0.2874	0.1696
FPP@PM-3	18	13.25	0.2586	0.1290
FPP@AM-1	33	18.65	0.2210	0.1099
FPP@AM-2	29	14.68	0.2515	0.1522
FPP@AM-3	17	13.57	0.2586	0.1479
FPP@A3-M1	40	14.84	0.1462	0.1070
FPP@A5-M1	32	11.00	0.1082	0.1091